Analyzing the seismic hazard of Jishishan earthquake based on multi-source data

Wei Li[1,2,3], Jinchen Du [1,2,3], Haowen Yan[1,2,3]

1. Faculty of Geomatics, Lanzhou Jiaotong University, Lanzhou 730070, China - geosci.wli@lzjtu.edu.cn, 11220870@stu.lzjtu.edu.cn, yanhw@mail.lzjtu.cn
2. National and Local Joint Engineering Research Center for Geographic Monitoring Technology Application, Lanzhou 730070, China
3. Key Laboratory of Science and Technology in Surveying & Mapping, Gansu Province, Lanzhou 730070, China

Keywords: Jishishan Earthquake, Seismic Hazard, Casualty Prediction, PSO-BiLSTM-Attention Model, Multi-source Data.

Abstract

An Ms6.2 earthquake occurred in Jishishan County, Linxia Hui Autonomous Prefecture, Gansu Province on December 18, 2023, which is another strong earthquake event that occurred in the eastern and northeast margin of the Qinghai-Tibet Plateau after the Ms6.8 Luding earthquake in 2022. To determine the spatial characteristics and human casualties of the earthquake, this paper obtains the seismic spatial information based on remote sensing data. The results show that the earthquake has thrust characteristics and is a thrust-type earthquake, in which the line-of-sight deformation of the lifting and falling rail coseismic deformation fields are mainly uplifted, 7.51cm, and 7.91cm respectively. At the same time, the PSO-BiLSTM-Attention population casualty model is proposed, and 149 people are predicted to die, which is 2 people less than the actual 151 people, indicating that the model can well estimate the post-disaster death toll and can be used for the post-disaster death population assessment.

1. Introduction

In the emergency response and rescue efforts following the Jishishan earthquake, geospatial information technology through surveying and mapping, remote sensing, which played a pivotal role. Upon the earthquake's occurrence, the natural resources departments swiftly activated emergency mapping support mechanisms, utilizing high-resolution satellites and unmanned aerial vehicles (UAVs) as remote sensing platforms to rapidly image and monitor the affected area. These technologies not only furnished vast, high-precision imagery data of both pre- and post-disaster conditions but also leveraged three-dimensional modelling techniques to construct detailed terrain and geomorphological models of the disaster zone, providing precise geographical information support to rescue teams.

Through remote sensing image analysis, rescue personnel were able to swiftly grasp the extent of damage in the disaster area, including road disruptions, collapsed buildings, and potential geological hazard sites, serving as a crucial foundation for formulating scientific rescue plans. Furthermore, thematic maps and three-dimensional simulation models based on geospatial information data facilitated robust support for disaster reconstruction planning, secondary disaster prevention, and other related endeavors.

Additionally, natural resources departments coordinated efforts with commercial satellite companies, geoinformation enterprises, and other stakeholders to collectively engage in the seismic region's surveying, remote sensing, and mapping work, fostering an efficient collaboration mechanism. These concerted efforts not only enhanced emergency mapping support capabilities but also amassed invaluable data and experiences for subsequent earthquake scientific research, disaster risk assessments, and related endeavors.

In summary, geospatial information technology through surveying and mapping, and remote sensing significantly contributed to the emergency response and rescue operations of the Jishishan earthquake, offering timely, accurate, and comprehensive geographical information support, safeguarding the lives and property of the affected populace.

2. Overview of the Study Area

Jishishan is located in the southwest of Gansu Province, with an administrative area of 909.97 km^2. The terrain is high in the southwest and low in the northeast. It has jurisdiction over 17 townships (towns), 145 administrative villages, and 7 community neighborhood committees (Figure 1(b)). By the end of 2022, the county's permanent population is 238,900, of which 55,100 are urban and 183,800 are rural, accounting for 76.94% of the county's permanent population.

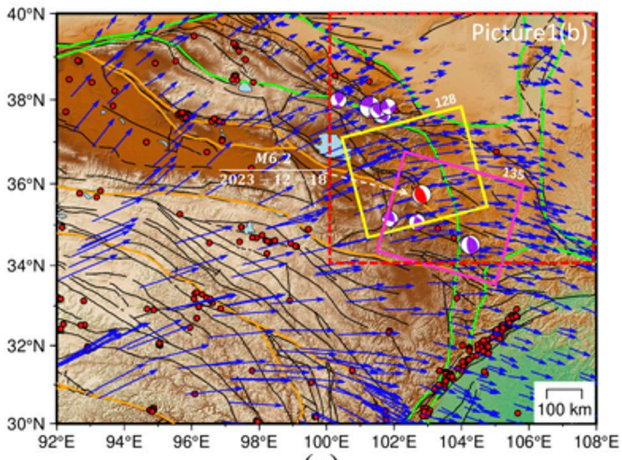

(a)

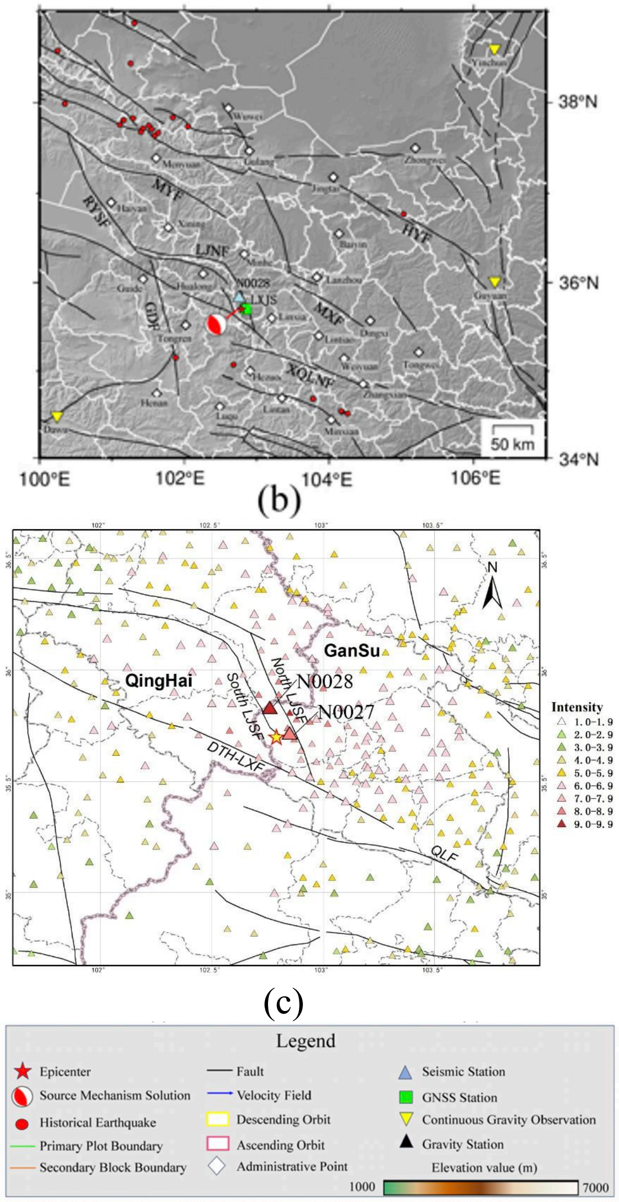

Figure 1. Structural sketch of the study area.

Figure 1(a) represents the tectonic background of the northeastern margin of the Qinghai-Tibet Plateau; Figure 1(b) represents the tectonic background and station location information of the ancient and modern area of Jishishan earthquake, in which MYF represents the Menyuan fault, RYSF represents the Riyueshan fault, LJNF represents the northern margin of Laji Mountain fault, HYF represents the Haiyuan fault, and GDF represents the GUI default. XQLNF represents the northern margin fault of the West Qinling Mountains, and MXF represents the Maxianshan fault. In addition, the purple beach ball in Figure 1(a) is the focal mechanism solution of the historical earthquake, and the red beach ball in Figure 1(a) and Figure 1(b) is the focal mechanism solution of the current earthquake. Source mechanism solutions from the United States Geological Survey (USGS, http://www.usgs.gov). Figure 1(c) encompasses the locations, quantity, distribution characteristics, and potential impacts of GNSS (Global Navigation Satellite System) stations. Additionally, let's delve into the relevant earthquake monitoring and early warning systems, as well as how they collaborate with GNSS stations to provide more accurate disaster warnings.

As shown in Figure 1, the fault distribution in the focal area of the Jishishan earthquake is complex. The earthquake takes place at the junction of Gansu Province and Qinghai Province and the northeast margin of the Qinghai-Tibet Plateau. In history, more than 20 destructive earthquakes of magnitude 5.0 or higher have occurred in this area; while the LJNF, LJSF, and XQLNF are developed in this study area. The Lajishan fault is the main fault running through Jishishan County, showing typical thrust structure characteristics. The results of GPS velocity field research show that the northeastern part of the Qinghai-Tibet Plateau is characterized by NE-trending lateral squeezing and crustal shortening, which is a sensitive area for earthquake breeding (Zhuang, 2023). The cause of this earthquake may be the squeezing action of the NE extension of the Qinghai-Tibet Plateau (Zhou, 2016; Zhuang, 2023).

3. Data and Methods

To study the space disaster situation of Jishishan, this paper analyzes the spatial characteristics of coseismic deformation obtained from Sentinel-1 satellite ascending and descending orbit radar images. At the same time, this paper also proposes a new method combining Particle Swarm Optimization (PSO), Bidirectional Long Short Term Memory (BiLSTM), and the neural network model of the Attention mechanism used to predict the casualties of the Jishishan earthquake.

3.1 Seismic Deformation Field Acquisition

The Jishishan earthquake is the largest earthquake to have occurred near the Lajishan fault zone since seismic records. Therefore, it is of great significance to extract the coseismic deformation field of the Ms6.2 Jishishan earthquake in 2023 for further understanding the spatial evolution process of the regional earthquake disaster population. This paper utilizes Envi5.6 and Sarscape5.6.2 to process both ascending and descending orbit data from Sentinel 1A satellites to obtain the coseismic deformation field of the Jishishan earthquake. The line of sight (LOS) deformation of the earthquake was obtained using the two-orbit method with data from the Sentry 1 radar satellite, as shown in Table 1.

Orbit	Number	Time	Time Interval	Polarization Mode	Data Mode	Spatial Resolution
Ascending	128	2023-10-27 2023-12-26	60 days	VV	IW	5 m×20 m
Descending	135	2023-12-14 2023-12-26	12 days	VV	IW	5 m×20 m

Table 1. Parameters of the sentinel-1 radar satellite used in this study.

As can be seen from Figure 2, the coseismic deformation fields of the ascending and descending rails both show an earlobe shape, and the deformation trend is parallel to the fracture trend of Lajishan. The results show that the earthquake caused obvious surface co-seismic displacement, and the co-seismic deformation field of lifting rail was mainly uplift deformation, and no clear and obvious surface settlement information was observed (Liu, 2024). The coseismic deformation field obtained from the ascending rail image is about 7.51cm along the line of sight, and the maximum settlement value is 5.11cm; the co-seismic deformation field obtained from the descending rail image is about 7.91cm along the line of sight, and the maximum settlement value is about 6.71cm (Li, 2024). These deformation characteristics reflect that the earthquake has the characteristics of reverse faults, and it is presumed that the earthquake occurred at an NNW trending eastern thrust blind fault (Li, 2024; Yang, 2024).

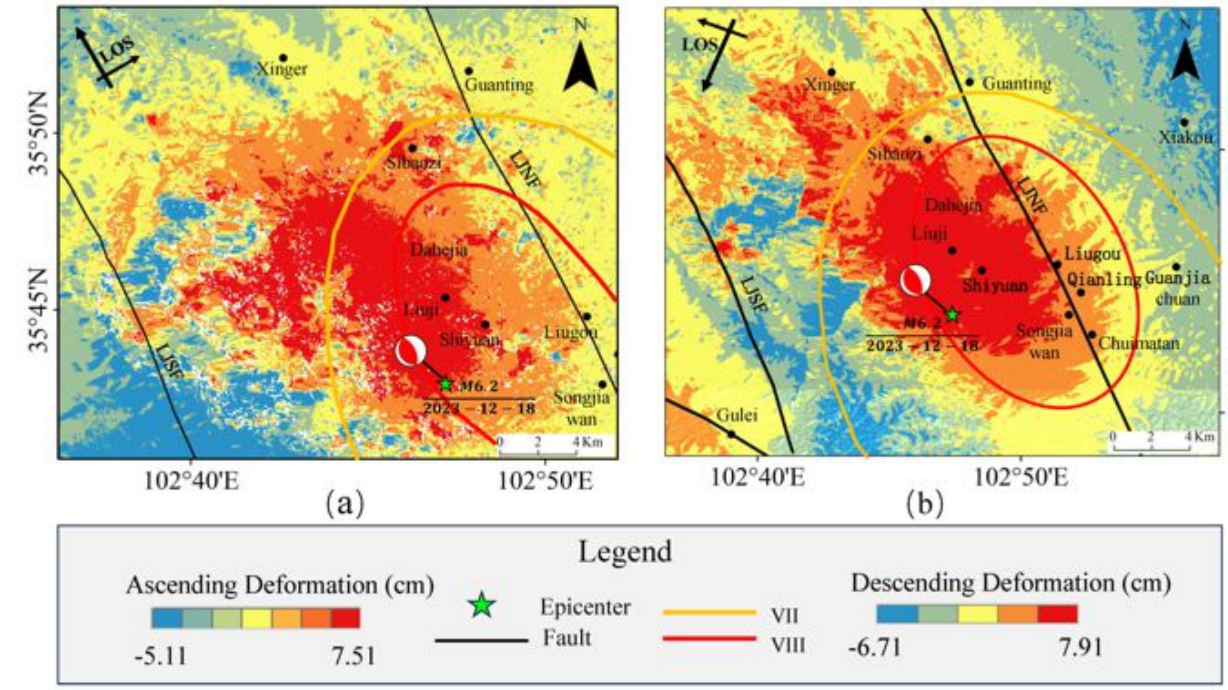

Figure 2. The coseismic deformation field of the Jishishan earthquake.

3.2 Population Casualty Model

According to the nonlinear and high-dimensional characteristics of earthquake casualty data, this paper constructs a prediction model based on the PSO of BiLSTM combined with Attention (PSO-BiLSTM-Attention). The model principle is shown in Figure 3.

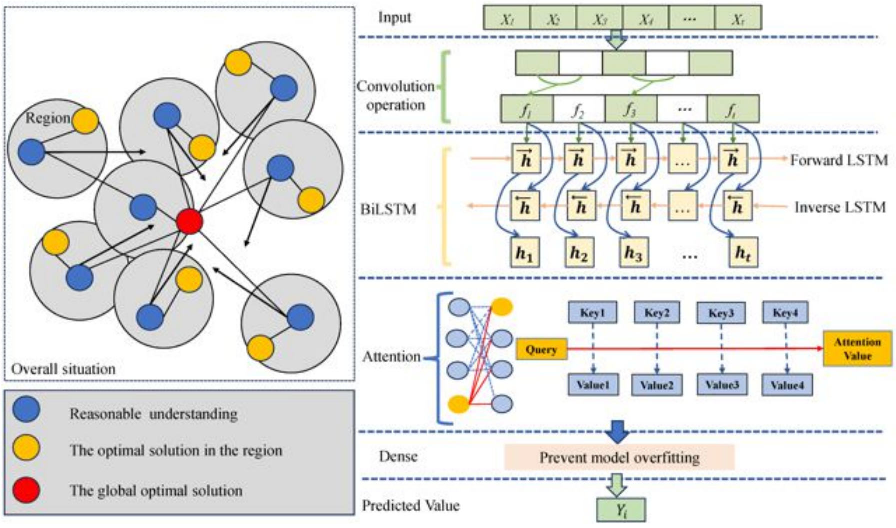

Figure 3. The coseismic deformation field of the Jishishan earthquake.

This research collects historical earthquake data from 1949 to 2021 for the nonlinear prediction of earthquake casualties. The missing values are supplemented, and the historical earthquake samples during this period are used as training and test samples. Seven parameters that significantly impact earthquake casualties are selected as input factors for the PSO-BiLSTM-Attention prediction model: earthquake time, magnitude, focal depth, epicenter intensity, protection grade, population density, and casualties (Chen, 2024). The earthquake time is categorized into three intervals (6 to 13:00, 13 to 21:00, and 21 to 6:00 the next day) represented by numbers 1, 2, and 3 (Zhou, 2017). Additionally, due to variations in earthquake strength and discontinuity leading to differences in casualty numbers, a separate normalization process is applied before inputting the data into the model to minimize its impact on predictions.

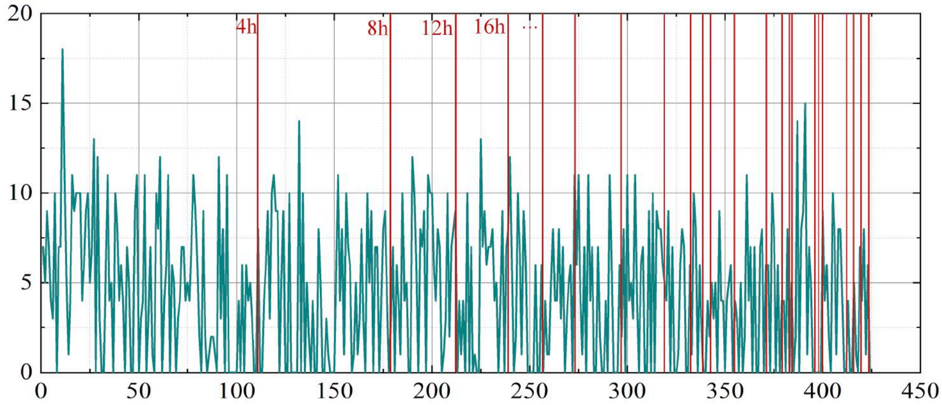

(a)

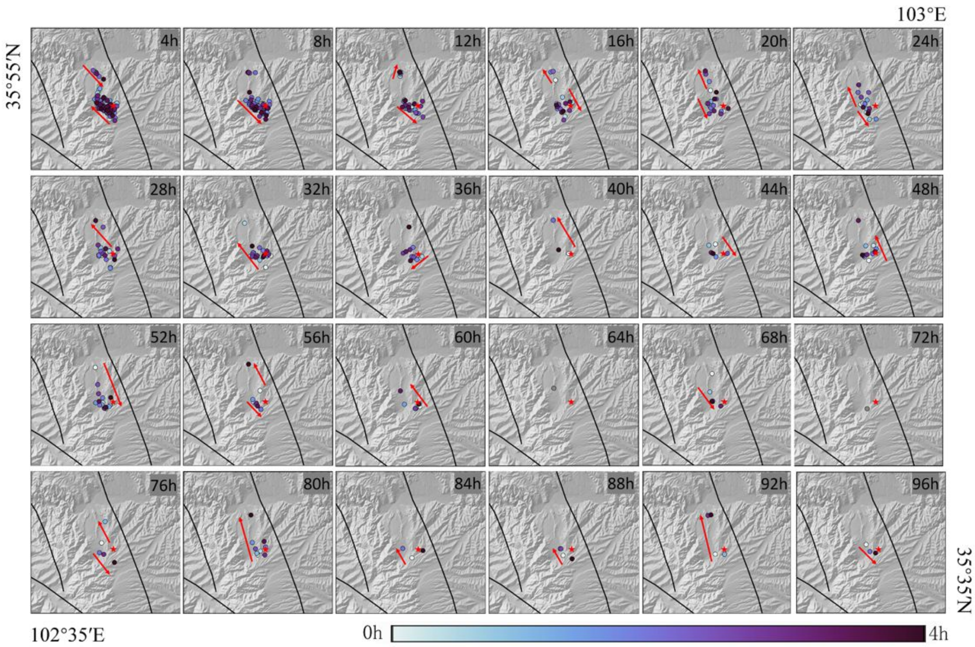

(b)

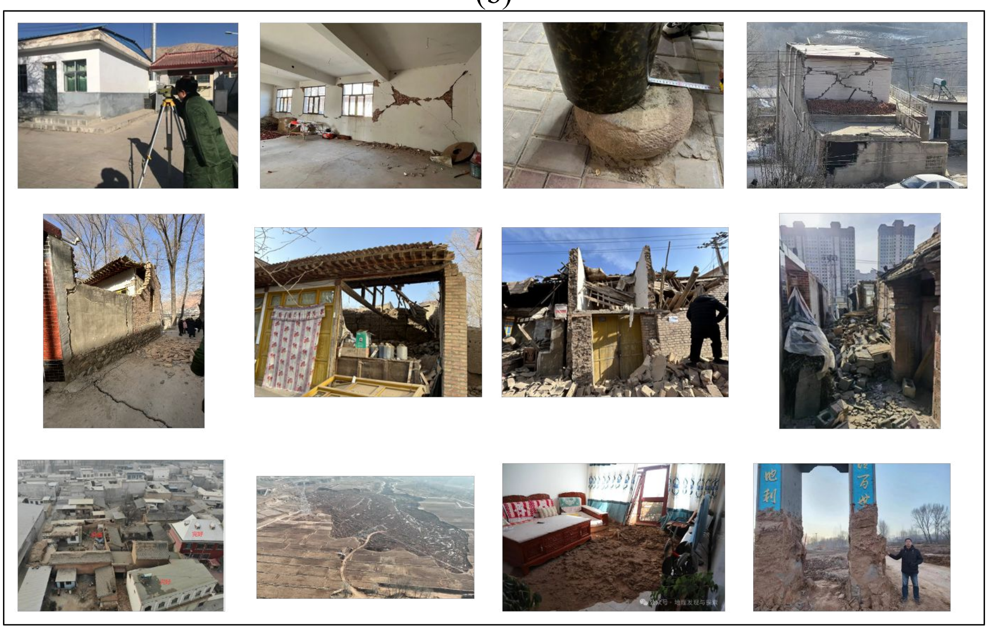

(c)

Figure 4. Jishishan earthquake aftershock time series and on-site investigation of damaged houses due to the earthquake disaster.

After the earthquake, the region entered a stage of frequent aftershocks. According to statistics over the following days, the number of aftershocks continued to rise, with hundreds of aftershocks recorded in total, including significant aftershocks of magnitude 3.0 and above (as shown in Figure 4(a) and Figure 4(b)). These aftershocks exhibited a dense and continuous pattern in time, with some occurring within minutes of each other and others separated by several hours, forming a complex earthquake time series. Earthquake departments and scientific researchers are closely monitoring these aftershock activities, assessing their impact on the local area through data analysis (Figure 4(c)), and providing scientific support for subsequent earthquake relief and disaster relief efforts.

The model is trained by distributing the training set and the test set in a ratio of 4:1. As depicted in Figure 5(a) and Figure 5(b), the overall trend of the prediction results is relatively stable, with some instances showing large peak values. This can be attributed to the presence of input samples containing earthquake cases with significant damage and higher casualties, resulting in a sharp increase in the predicted number of casualties within the output population. However, this has minimal impact on model accuracy. The predicted R^2 for the test set and training set were 0.96387 and 0.9898 respectively, while RMSE values were 0.83086 and 0.55977 respectively, indicating a strong training effect. The MAE values were found to be 0.58354 for the test set and 0.33742 for the training set, further confirming an effective training process. By inputting relevant factors of the Jishishan earthquake into our trained PSO-BiLSTM-Attention model for prediction purposes, we estimated that there would be approximately 149 deaths as a result of this event only two people different from the actual value of 151 people. This represents an accuracy rate of 98.45% and an error rate of 1.54%.

To verify the accuracy of the model, the Nepal earthquake, Tangshan earthquake, Xingtai earthquake, Luhuo earthquake, and Wenchuan earthquake are selected as the verification set. As can be seen from the results of the verification set of earthquake cases in Table 2, the error distribution ranges from 0.47%-6.1%, and the average error is 3.06%, indicating that the model can well estimate the post-disaster death toll and can be used for the post-disaster death population assessment.

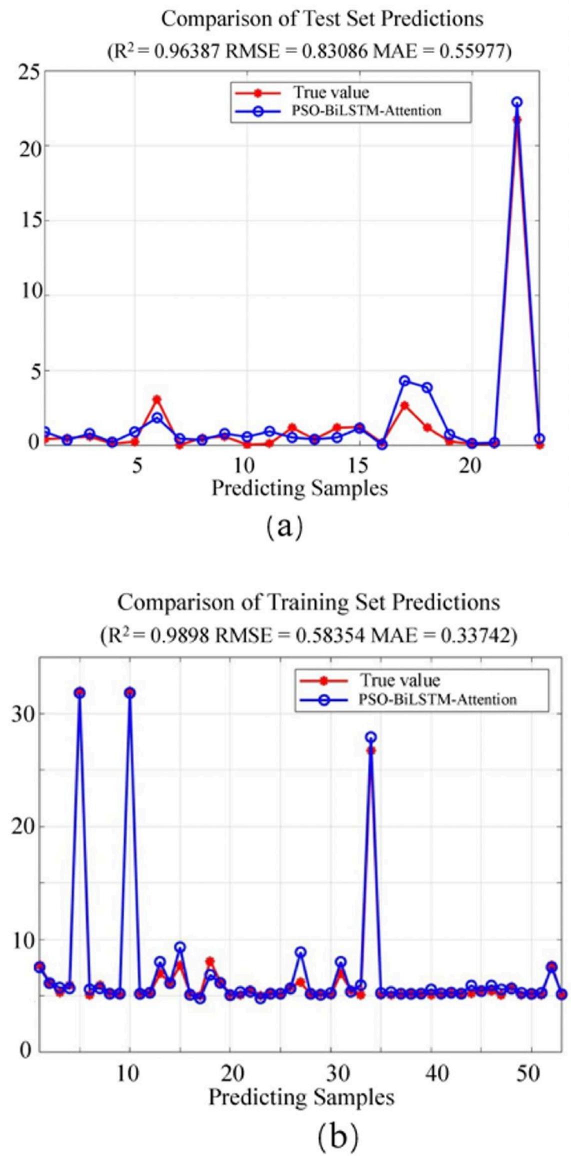

Figure 4. The result of the model prediction.

Earthquake Examples	Output Results (People)	True Value (People)	Error Value (People)	Error Rate (%)
M8.1 Nepal	8250.005	8786	-535.995	6.10
M7.8 Tangshan	240842.687	242000	-1157.31	0.48
M7.2 Xingtai	7982.808	8064	-81.192	1.01
M7.6 Luhuo	15073.029	15621	-547.971	3.51
M8.0 Wenchuan	72139.598	69227	+2912.598	4.21
M6.2 This earthquake	148.673	151	-2.327	1.54

Table 2. Model validation set results.

4. Result

(1) New technologies in surveying and mapping, remote sensing, and geographic information systems (GIS) play a crucial role in earthquake disaster research. By providing high-precision and timely geospatial data, they offer robust support for earthquake disaster monitoring, assessment, rescue, and reconstruction efforts.

(2) The co-seismic deformation field is located between the southern and northern edges of Laji Mountain, and the main uplift area is 15 km×15 km, concentrated near the epicenter. The co-seismic deformation field of the lifting rail increases by about 7.51cm and 7.91cm along the line of sight. The distribution of the aftershocks of the earthquake was linear in the direction of NW to SE, and the general trend was parallel to the strike of the Laji Mountain fault. It can be inferred that the earthquake may have occurred in a north-northwest or south-southeast strike of the earthquake fault.

(3) By constructing the PSO-BiLSTM-Attention prediction model, the death toll of the Jishishan earthquake was predicted. The prediction result was 149 people, the accuracy was 98.45%, and the error was 1.54%. Moreover, the average error of the model is 3.06%, which is only 2 people less than the actual

result of 151. It shows that the model can predict the casualties well and can be used to evaluate the dead population after the disaster.

Acknowledgements

This work is supported by the National Natural Science Foundation of China (Grant No. 41930101), the China Postdoctoral Science Foundation (Grant No. 2019M660091XB), the Natural Science Foundation of Gansu Province (Grant Nos. 23JRRA857, 23JRRG0015, and 21JR7RA317), the Youth Doctor Support Program of Colleges and Universities in Gansu Province (Grant No. 2024QB-046); the Open Fund Project of the National Glacier, Permafrost, and Desert Scientific Data Center (Grant No. E01Z790201/2021kf07), the Lanzhou Talent Innovation and Entrepreneurship Support Project (Grant No. 2022-RC-73), the Key Project of Experimental Teaching Reform of Lanzhou Jiaotong University (Grant No. 2024002), and the "Young Scientific and Technological Talents Support Program" of Gansu Province (Li Wei). Thank the European Space Agency for providing Sentinel-1A Sentinel data (https://asf.alaska.edu/). The regional seismic waveform data used in this study comes from the "National Digital Seismic Network Data Backup Center" of the Institute of Geophysics, China Earthquake Administration. The regional seismic gravity data comes from the research team led by Zhao Yunfeng from the Second Monitoring Center of China Earthquake Administration. The precise location results of this earthquake sequence come from the research team led by Zhao Cuiping from the Earthquake Prediction Research Institute of China Earthquake Administration. Most of the figures in this article were created using GMT (Wessel P, et al., 2019). My deepest gratitude goes to them all.

References

Chen S.J., Liu Z.W., Zhou H., 2024: Research on prediction of earthquake death toll based on PCA-PSO-ELM model. *Journal of Geodesy and Geodynamics*. 44(1): 105-110.

Li W., Du J.C., Zhang C., et al., 2024: Research on spatiotemporal evolution of disaster and population casualties in Jishishan earthquake by fusing multi-source data. *Geomatics and Information Science of Wuhan University*.

Liu Z.J., Han B.Q., Nai Y.H., 2024: Source parameters and slip distribution of the 2023 Mw 6.0 Jishishan (Gansu, China) earthquake constrained by InSAR observations. *Geomatics and Information Science of Wuhan University*.

Li Y.S., Li W.L., Xu Q., 2024: Coseismic deformation and slip distribution of the 2023 Jishishan Ms6.2 earthquake revealed by InSAR observations. *Journal of Chengdu University of Technology (Science & Technology Edition)*. 1-13.

Li W.L., Xu Q., Li Y.S., 2024: Preliminary analysis of the coseismic geohazards induced by the 2023 Jishishan Ms 6.2 earthquake. *Journal of Chengdu University of Technology (Science & Technology Edition)*. 1-16.

Wessel P., Luis J.F., Uieda L., et al., 2019: The generic mapping tools version 6. *Geochemistry, Geophysics, Geosystems*. 20(11): 5556-5564.

Xu Q., Peng D.L., Fan X.M., et al., 2024: Preliminary study on the characteristics and initiation mechanism of Zhongchuan town flowslide triggered by Jishishan Ms 6.2 earthquake in Gansu province. *Geomatics and Information Science of Wuhan University*. 1-18.

Yang J.Y., Wen Y.M., Xu C.J., 2024: Seismogenic fault structure of the 2023 Jishishan (Gausu) Ms6.2 earthquake revealed by InSAR observations. *Geomatics and Information Science of Wuhan University*. 1-11.

Zhuang, W.Q., Cui D., Hao M., 2023: Geodetic constraints on c ontemporary three-dimensional crustal deformation in the Laji S han—Jishi Shan tectonic belt. *Geodesy and Geodynamics*, 14(6): 589-596.

Zhou D.H., Feng H., Cheng L.Q, 2017: On the relation between the psychological empowerment and the violation behaviours of the airport security staff members. *Journal of Safety and Environment*. 17(6): 2267-2272.

Zhou L., Wang Q.L., Li Z.J., 2016: The study of crustal deformation on western end of Lajishan fault based on GPS and levelling data. *Journal of Geodesy and Geodynamics*. 36(12): 1056-1060.